

## Surface superconductivity in niobium and niobium-tantalum alloys\*

J. R. Hopkins<sup>†</sup> and D. K. Finnemore

Ames Laboratory-USAEC and Department of Physics, Iowa State University of Science and Technology, Ames, Iowa 50010

(Received 16 July 1973)

The critical field for surface superconductivity,  $H_{c3}$ , and the upper bulk critical field,  $H_{c2}$ , have been measured as a function of temperature and mean free path for Nb and Nb(Ta) alloys in an attempt to study the spatial variations of the superconducting interaction constant  $N(0)V$  near a vacuum-metal interface. At temperatures below  $T/T_c = 0.85$ , the pure-Nb sample shows  $H_{c3}/H_{c2}$  values well above 1.695, as predicted by Hu and Korenman for the limit of long electronic mean free path. As the mean free path decreases, there is a regular depression of  $H_{c3}/H_{c2}$  toward 1.695. At temperatures above  $T/T_c = 0.85$ , however, there are striking deviations from the theory which may arise because the interaction constant is slightly depressed at the surface. A model calculation by Hu shows that changes in  $N(0)V$  at the surface of 0.7% for pure Nb and 1.6% for Nb-1.0-at.% Ta can account for the experimental results.

### INTRODUCTION

The theory of surface superconductivity<sup>1,2</sup> agrees with experiment<sup>3</sup> rather well for temperatures well below the transition temperature  $T_c$ . Shortly after Saint James and de Gennes<sup>1</sup> first predicted the existence of surface superconductivity, several experiments<sup>3</sup> confirmed that the ratio of the critical fields ( $H_{c3}/H_{c2}$ ) was about 1.7, in accord with theory, and the basic idea of surface superconductivity quickly became well established. Indeed, extensions of the original theory to cover the case of materials with long mean free paths also agree with experiment<sup>4,5</sup> at low temperature. At temperatures very close to  $T_c$ , however, several investigators<sup>5-7</sup> have observed systematic deviations from the theory which are far outside experimental error. Soon after the discrepancies were found, Hu<sup>8</sup> suggested that the deviations could be explained by a spatial variation of the strength of the interaction parameter,  $N(0)V$ ,<sup>9</sup> and he performed model calculations which showed that the data could be fit rather well if  $N(0)V$  changes by as little as a few percent for a distance comparable to the coherence distance at  $T=0$ ,  $\xi(0)$ , near the surface. The purpose of this work is to test the Hu model for a wide range of normal-state mean free paths  $l$ . If the Hu explanation is correct then the temperature dependence of  $H_{c2}$  and  $H_{c3}$  can be used as a tool to study the spatial dependence of  $N(0)V$  near a vacuum-metal interface.

### EXPERIMENTAL

#### Sample preparation

Dissolved gases strongly affect the superconducting properties of Nb so an important aspect of this research is the removal of these gases and the preparation of clean surfaces. Some time ago De Sorbo<sup>10</sup> showed that dissolved oxygen can depress  $T_c$  of Nb by 0.93 K per at.% oxygen, and

it can lead to rather broad transitions. Fortunately most of the dissolved gases can be removed from Nb and clean surfaces can be prepared by outgassing at temperatures near the melting point in a high vacuum. Hence the general approach adopted here is to heat the sample by electron bombardment to a temperature of about 2000 °C for several hours in a vacuum of  $10^{-9}$  Torr and then to cool the sample and seal it in a Pyrex tube without exposure to air. Most of the samples were prepared in this way but some were subsequently anodized.

The Nb metal used in this work was obtained from the Du Pont Corp. (Lot No. CDH-43-9). To prepare the samples, pure Nb was arc melted and then electron-beam melted into a button about 3.75 cm in diameter. This button was then cut into pieces and arc melted with appropriate quantities of Ta to form the alloys. Each of these buttons was then swaged and drawn into 0.075-cm-diam wires, electropolished in a 2% sulfuric-acid-methanol mixture at  $-70$  °C for 5 min, and cut into 3.75-cm-long pieces. Near one end of this wire, a 0.63-cm segment was rolled into a ribbon approximately 0.013 cm thick and 0.075 cm wide. The purpose of this was to provide a region where the sample could be melted easily to separate the desired portion of the sample from the spot-welded section after outgassing. If this section were not thin then the surface tension is larger than the weight of the sample and the wire melts into a ball rather than dropping into the Pyrex capillary, shown in Fig. 1.

To outgas the sample, the flattened end of the wire was spot welded to a tungsten electrode and mounted in a high-vacuum electron-bombardment apparatus shown in Fig. 1. Normally the sample was heated to about 2000 °C in a vacuum of about  $2 \times 10^{-9}$  Torr. At this temperature and pressure, the absorption and evaporation rates give a sample

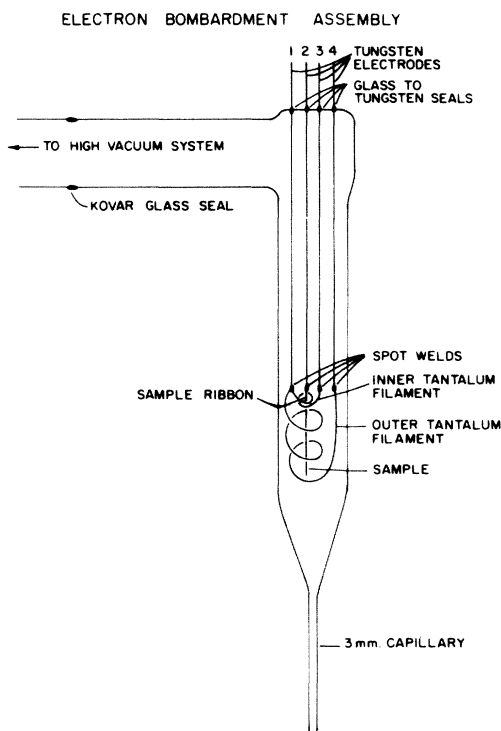


FIG. 1. Electron-bombardment apparatus for outgassing the samples and cleaning the surface. After sample preparation, the thin-ribbon section near the top was melted and the sample dropped into the capillary.

with concentrations of a few ppm N and O.<sup>11</sup> After 24 h at 2000 °C the power was abruptly stopped and the sample cooled to less than 500 °C in less than 2 sec. After the sample had cooled 2 to 3 h in the high vacuum, a small filament wrapped around the ribbon section of the wire was used to melt the wire and separate the sample from the electrode. The sample then dropped into a capillary tube. The vacuum pump was then shut off and the system was filled with 99.999%-pure-He gas to a pressure of about 600 Torr. The sample was then sealed inside the glass capillary with a torch.

Results of the analyses of the samples made after the superconducting measurements are shown in Table I. Ta and W were determined by neutron activation to better than 10%. N, O, and H were determined to about 10% by mass fusion. Other trace impurities were determined by mass spectroscopy. The only element for which a good analysis was not made was carbon, but previous work<sup>12</sup> indicates that the carbon content should be less than 100 at. ppm.

#### Cryostat

The apparatus used in this work was a conventional heat-leak chamber suitable for use between

1 and 20 K. To ensure thermal equilibrium, the sample, the pickup coils, and the thermometers were mounted in a brass yoke which was then mounted inside a sealed brass can. This whole interior assembly was then exposed to He<sup>4</sup> gas at a pressure of 0.2 Torr to aid the thermal equilibrium. This inner can was then isolated from the liquid-He<sup>4</sup> bath by an evacuated chamber in the usual way. Temperature stability of 0.0001 K was routinely maintained for period of 5 min and stability of 0.001 K was maintained for several hours as needed. Values of the temperature were determined by the same germanium thermometer (GR 99) used in earlier work.<sup>12</sup>

The primary dc magnetic fields were generated by a liquid-nitrogen-cooled solenoid which was calibrated by proton resonance in glycerine to give  $152.45 \pm 0.02$  Oe/A for 6 different fields between 1700 and 3300 Oe. The power supply for the magnet was a Spectromagnetic current-regulated supply which was stable to one part in  $10^5$  for periods of several hours. The earth's magnetic field was compensated to approximately 0.01 Oe by Helmholtz coils. Mutual-inductance coils for the ac susceptibility measurements were wound astatically on nylon forms and oriented so that the ac exciting field and the steady dc field of the liquid-nitrogen-cooled solenoid were parallel to the axis of the cylindrical sample.

## RESULTS AND DISCUSSION

### Permeability curves

The general shapes of the magnetic field dependence of the real and imaginary parts of the permeability ( $\mu'$  and  $\mu''$ ), as shown on Fig. 2, are similar to the results reported earlier.<sup>4,5</sup>  $H_{c1}$  was defined as the field where  $\mu'$  is half-way up the first peak, and  $H_{c2}$  was taken to be the high-field shoulder of the second peak. These identifications agree well with magnetization data<sup>12</sup> and are reproducible from sample to sample. Above  $H_{c2}$ ,  $\mu'$  monotonically approaches the normal-

TABLE I. Results of the chemical analyses for several samples (at. ppm).

| Sample                              | Ta     | O  | N  | H  | Fe | W  |
|-------------------------------------|--------|----|----|----|----|----|
| H-7, Nb                             | 43     | 13 | <1 | <1 | 5  |    |
| H-9, Nb <sup>a</sup>                | 110    |    |    |    |    | 48 |
| H-26, Nb <sup>a</sup>               |        |    |    |    |    |    |
| H-15, Nb-1 000-ppm Ta               | 730    | <1 | <1 | <1 | 10 | 44 |
| H-19, Nb-1 000-ppm Ta <sup>a</sup>  | 1150   |    |    |    |    |    |
| H-13, Nb-5 000-ppm Ta <sup>a</sup>  | 5 590  |    |    |    |    |    |
| H-21, Nb-5 000-ppm Ta               | 6 320  | 5  | <1 | <1 | 5  | 48 |
| H-10, Nb-10 000-ppm Ta              | 10 300 | 60 | <1 | <1 | 1  | 48 |
| H-11, Nb-10 000-ppm Ta <sup>a</sup> | 10 600 |    |    |    |    |    |
| H-23, Nb-20 000-ppm Ta <sup>a</sup> | 22 100 |    |    |    |    |    |
| H-27, Nb-20 000-ppm Ta              | 25 100 | 6  | <1 | <1 | 10 | 43 |

<sup>a</sup>Samples used for ac susceptibility measurements.

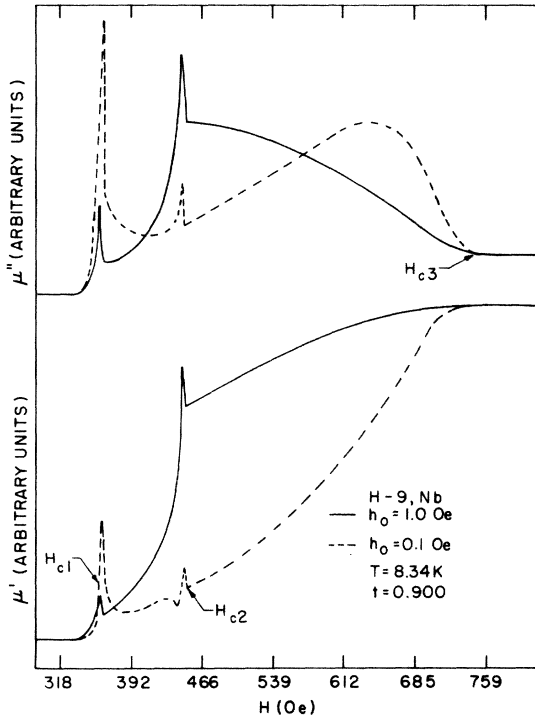


FIG. 2. Permeability curves for pure Nb at two different measuring fields.

state value, whereas  $\mu''$  either goes through a maximum or monotonically approaches the normal-state value depending on the value of the ac measuring field.  $H_{c3}$  is somewhat more difficult to define than  $H_{c1}$  and  $H_{c2}$  because there is considerable rounding.<sup>13</sup> The critical-current model for the surface sheath discussed by Rollins and Silcox<sup>14</sup> suggests that  $\mu''$  curves give a more sensitive measurement of  $H_{c3}$  and we find this to be the case for these samples. Hence  $H_{c3}$  was taken as the intersection of straight-line portions of the  $\mu''$  curve above and below  $H_{c3}$ .

Several factors which can alter the detailed shape of the  $\mu'$  and  $\mu''$  curve were studied in some detail. As shown in Fig. 2, the magnitude of the peaks at  $H_{c1}$  and  $H_{c2}$  change substantially as the magnitude of the ac measuring field,  $h_0$ , is varied, but the values of  $H_{c2}$  and  $H_{c3}$  do not change. At fields above  $H_{c2}$  the peak in  $\mu''$  shifts to lower fields with increasing  $h_0$ , as predicted from the critical-current model.<sup>14</sup> Values of the critical shielding currents  $J_c$  shown on Fig. 3 are about 0.2 A/cm at  $H_{c2}$ . These values are somewhat smaller than earlier measurements with Pb-In alloys<sup>14</sup> but larger than values for Ti-Nb alloys.<sup>15</sup> No adequate theory yet exists to explain the small magnitude of  $J_c$ .<sup>16</sup>

Two other factors which might influence the

phase boundaries were sample alignment and hysteresis on the  $\mu'$ -vs- $H$  plots. Small errors in aligning the sample axis with the applied field<sup>14</sup> can make substantial changes in the  $\mu'$  and  $\mu''$  curves, but the values of  $H_{c1}$ ,  $H_{c2}$ , and  $H_{c3}$  are not changed by more than 1% as long as the alignment is within  $1^\circ$ . Misalignments up to  $3^\circ$  were studied.

Between  $H_{c2}$  and  $H_{c3}$ , the magnitudes of the  $\mu'$  and  $\mu''$  for increasing values of the dc magnetic field are essentially the same as those for decreasing  $H$  so that there is little hysteresis in the  $\mu'$ - or  $\mu''$ -vs- $H$  plots in this region. Between  $H_{c1}$  and  $H_{c2}$ , however, the field-decreasing  $\mu'$  plots lie much closer to the normal-state values than the field-increasing  $\mu'$  plots and the magnitude of this effect varies from sample to sample. This effect was too irreproducible to warrant a thorough study. The values of  $H_{c1}$  and  $H_{c2}$ , however, do not change even though the hysteresis changes. Detailed discussions of these effects are available elsewhere.<sup>13</sup>

For pure Nb and the 5000-ppm-Ta sample the superconducting-to-normal transitions are 0.004 and 0.006 K wide, respectively, so the samples are rather homogeneous. In addition, the shape of the  $\mu'$ -vs- $H$  and  $\mu''$ -vs- $H$  curves remain unchanged right up to a reduced temperature of  $t=0.996$ , providing  $h_0$  is sufficiently small. This is similar to results reported earlier<sup>4</sup> for a different pure-Nb sample. For the 10000-ppm alloy, however, the zero-magnetic-field transitions are nearly 0.040 K wide and there is some broadening of the  $\mu'$ -vs- $H$  curves for all temperatures above  $t \approx 0.96$ . This effect then limits the temperature range over which measurements are meaningful for this sample to temperatures below  $t=0.96$ .

#### Vortex state characteristics

For all the samples reported here, the vortex-state parameters agree well with the Ginsburg-

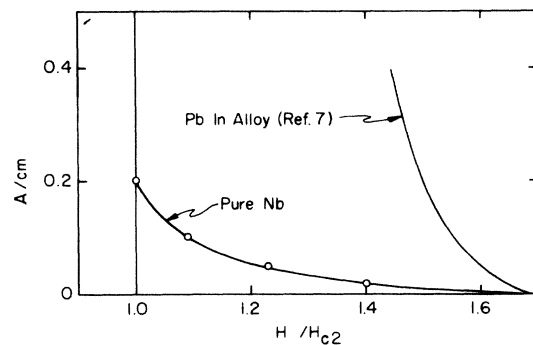


FIG. 3. Critical currents deduced from the maximum in the  $\mu''$  vs  $H$  curve.

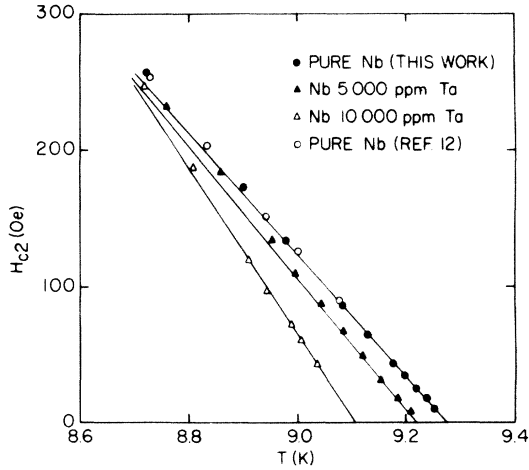


FIG. 4. Temperature dependence of  $H_{c2}$  near  $T_c$ .

Landau theory near  $T_c$ .<sup>17</sup> As shown in Fig. 4,  $H_{c2}$  has a linear temperature dependence with a slope which increases with increasing Ta content. The increase in slope is expected, of course, because the Ginsburg-Landau parameter  $\kappa$  increases. To determine the numerical value of  $\kappa$  for each sample, the measured normal-state resistivity  $\rho_n$  was used in conjunction with the equation  $\kappa = k_0 + (7.53 \times 10^3) \rho_n \gamma^{1/2}$ , where  $k_0$  is a constant equal to 0.76,<sup>12</sup>  $\rho_n$  is measured in  $\mu\Omega$  cm, and  $\gamma$  is the specific-heat coefficient measured in  $\text{erg}/\text{cm}^3 \text{K}$ .<sup>2</sup> In addition, one can calculate the London penetration depth at  $T=0$ ,  $\lambda_L(0)$ , from the relation<sup>18</sup>

$$\lambda_L(0) = \left[ \frac{\pi\sqrt{2}}{\varphi_0 \kappa} \frac{dH_c}{dt} \right]^{-1/2},$$

where  $\varphi_0$  is the flux quantum equal to  $2.07 \times 10^{-7}$  G cm<sup>2</sup>. One can also calculate the coherence distances  $\xi_0$  from

$$\xi_0 \cong 0.96 \lambda_L(0) / \kappa$$

if we assume that all these samples are essentially in the clean limit. Values of each of these parameters are given in Table II for four different values of  $x$ , the Ta concentration.

#### Surface superconductivity

For temperatures below a reduced temperature,  $t = T/T_c$ , of 0.7 the data agree rather well with the original theories,<sup>1,2</sup> as shown on Fig. 5. The ratio of  $H_{c3}/H_{c2}$  for pure Nb lies between the pure-limit Hu and Korenman (HK) theory shown by the dotted line and the dirty-limit Saint James and de Gennes (SJDG) theory shown by the dashed line. Indeed, as the sample is made dirtier by adding Ta,  $H_{c3}/H_{c2}$  approaches the dirty limit.

For temperatures near  $T_c$ , however, the data deviate sharply from the theory<sup>1,2</sup> and approach 1.0 rather than 1.695. This is a very large effect which can clearly be seen from the  $\mu''$ -vs- $H$  curves of Fig. 6. Here, the data are plotted in terms of the reduced field  $H/H_{c2}$  to emphasize the large decrease in  $H_{c3}/H_{c2}$  as the temperature approaches  $T_c$ . There are some small changes in the shape of these  $\mu''$  curves which arise because the ratio of the measuring field  $h_0$  to  $H_{c2}$  changes, but basically the curves have the same shape and there is no difficulty identifying either  $H_{c2}$  or  $H_{c3}$ .  $H_{c3}/H_{c2}$  systematically falls well below 1.695 and approaches 1.0 as  $T$  goes to  $T_c$ .

A number of variables have been systematically changed to search for the origin of this effect. The coherence distance has been lowered by adding Ta and the deviations from the theory, as shown on Fig. 5, occur at successively lower temperatures. Qualitatively, however, the behavior is similar to pure Nb. A study was also made of a pure-Nb sample which had been anodized after the standard outgassing and the results are almost identical to the vacuum-cleaned surface, as shown by the diamonds of Fig. 5. In an earlier work a study also was made of samples

TABLE II. Sample characteristics for the Nb(Ta) alloys.

| $x$ (ppm Ta)                    | 100         | 1 000       | 5 000       | 10 000      |
|---------------------------------|-------------|-------------|-------------|-------------|
| $T_c$ (K)                       | 9.273       | 9.259       | 9.226       | 9.079       |
|                                 | $\pm 0.002$ | $\pm 0.002$ | $\pm 0.003$ | $\pm 0.020$ |
| $\rho$ ( $\mu\Omega$ cm)        | 0.009 06    | 0.0525      | 0.0967      | 0.38        |
| $\kappa$                        | 0.78        | 0.88        | 0.98        | 1.64        |
| $\lambda_L(0)$ ( $\text{\AA}$ ) | 3.14        | 334         | 353         | 456         |
| $\xi(0)$ ( $\text{\AA}$ )       | 387         | 364         | 343         | 268         |
| $l$ ( $\text{\AA}$ )            | 120 000     | 21 000      | 11 000      | 2900        |
| $D/\xi(0)$                      | $\sim 2.3$  | $\sim 2.3$  | $\sim 2.3$  | $\sim 2.3$  |
| $V_1/V_1$                       | 0.0076      | 0.0080      | 0.0096      | 0.016       |
| $Z'$                            | 0.039       | 0.040       | 0.049       | 0.078       |
| $H_{c3}/H_{c2}$ ( $T=0$ )       | 1.888       | 1.886       | 1.878       | 1.846       |
| $\xi(0)/b$                      | 0.019       | 0.022       | 0.029       | 0.044       |
| $\xi(0)/\kappa b$               | 0.025       | 0.025       | 0.029       | 0.027       |

exposed to air and again the results were similar to the Ta alloys. Every sample we have measured behaves much like the samples shown in Fig. 5. These deviations from the theory are very large and are well outside experimental uncertainty or errors in defining  $H_{c2}$  or  $H_{c3}$ .

One very reasonable model which can explain these results has been presented by Hu.<sup>8</sup> He has suggested that the rapid depression of  $H_{c3}$  near  $T_c$  arises because the superconducting interaction constant  $N(0)V$  is slightly depressed near the surface and he has worked out the temperature dependence of  $H_{c3}/H_{c2}$  for the case where  $N(0)V$  is depressed by a constant amount,  $N(0)V_1$ , for a distance  $D$  from the surface. The two important dimensionless parameters in the model then are  $D/\xi(0)$ , which measures the range of the perturbed interaction, and  $N(0)V_1/N(0)V$ , which measures the strength of the perturbation. To fit the results numerically one divides the data into three temperature regions depending on the relative size of the temperature-dependent coherence distance  $\xi(T)$  and  $D$ . At low temperatures (region A)<sup>8</sup> the thickness of the sheath is less than  $D$  and  $H_{c3}/H_{c2}$  is depressed below the HK theory<sup>2</sup> by a constant amount given by

$$\delta h = \frac{3.85 V_1/V}{N(0)V},$$

where

$$\delta h \equiv H_{c3}/H_{c2} \Big|_{\text{HK}} - H_{c3}/H_{c2} \Big|_{\text{data}}.$$

At intermediate temperatures (region B),<sup>8</sup> for which  $\xi(t)$  is greater than  $D$  but not much greater than  $D$ , Hu predicts

$$\delta h = z' \epsilon^{-1/2},$$

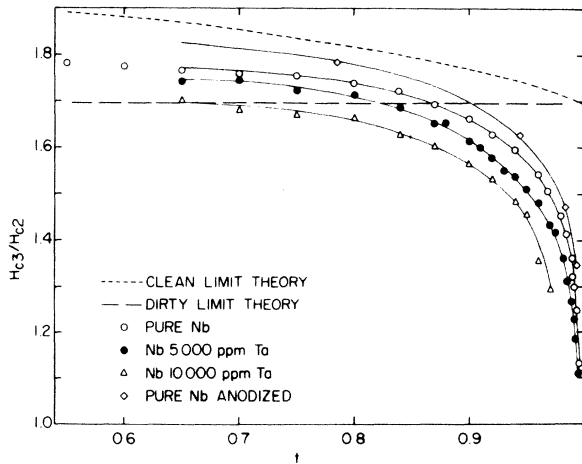


FIG. 5. Temperature dependence of  $H_{c3}/H_{c2}$  for a variety of samples. The clean-limit curve is from the HK theory and the dirty-limit curve is from the SJDG theory.

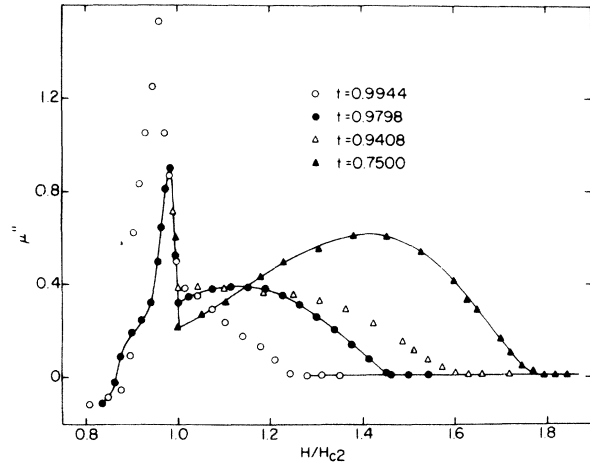


FIG. 6. Magnetic field dependence of  $\mu''$  at several different temperatures.

where  $\epsilon^{-1/2} = (1-t)^{-1/2}$  is the divergent factor for  $\xi(t)$  and

$$Z' = \frac{2.007}{N(0)V} \left( \frac{-V_1}{V} \right) \frac{D}{\xi(0)}$$

is a constant characteristic of the material. In the limit where  $\xi(T) \gg D$  (region C),  $\delta h$  does not approach infinity but approaches 0.695 as the broad sheath sees an average interaction constant which approaches the bulk value.

To see how well the model fits the data, we have plotted  $\delta h$  for several samples vs  $\epsilon^{-1/2}$  on Fig. 7. For  $t > 0.8$  all the samples show approximately a straight line with somewhat different slopes, and all the samples approach  $\delta h = 0.695$  as expected. All of the samples change behavior rather dramatically at  $t \approx 0.8$  or  $\epsilon^{-1/2} = 2.3$ , and we take this to be the boundary between region A and region B. Within the model this is the temperature for which the sheath thickness is equal to  $D$ ; so we would predict that  $D \approx 2.3 \xi(0)$  for all of these samples. This means that the range of the perturbed interactions scales with the  $T=0$  value of the coherence distance. From the values of the slope  $Z'$  one can also calculate that the magnitude of the perturbation varies from 0.76% for pure Nb to about 1.6% for the 10 000-ppm-Ta alloy. Values of all these parameters are summarized in Table II. This is a very small perturbation. Apparently the rather large changes in the electron-phonon interaction which might take place at the surface of a metal are averaged out in their effect on the superconducting order parameter so that the average effect is only about 1% over a rather substantial distance of about  $2.3 \xi(0)$ .

Another way to parametrize the data would be to arbitrarily adjust the slope of the wave function<sup>17</sup>

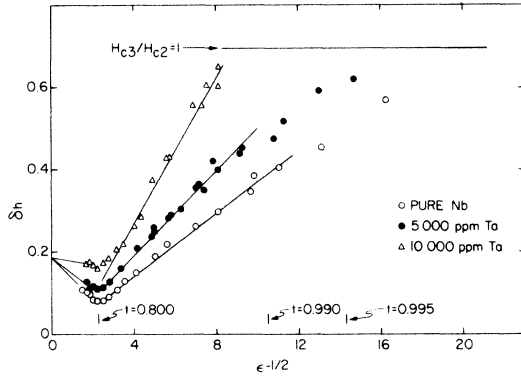


FIG. 7. Graphical fit of the data to the Hu model.  $\delta h$  is the deviation of the data from HK and  $\epsilon = 1 - t$ .

at the vacuum-metal interface to give the measured value of  $H_{c3}/H_{c2}$ . There is no full theory to convert  $H_{c3}/H_{c2}$  measurements into an effective slope

$$b = \frac{1}{\Psi} \frac{\partial \Psi}{\partial x},$$

but with the calculations of Fink and Joiner<sup>19</sup> as a guide one can estimate the ratio of  $\xi(0)/b$  to range from 1.9% for pure Nb to 4.4% for the 10 000-ppm-Ta sample. It is interesting to note that  $\xi(0)/b\kappa$  is very nearly a constant, but at present we do not understand this observation. A very small change in the slope of the order parameter can make drastic changes in the magnetic field range of sheath superconductivity near  $T_c$ . Hence the condition of the surface which governs the boundary condition on the superconducting wave function must be carefully controlled. Small amounts of metallic NbO<sup>20</sup> on the surface, for example, could make important changes in the slope of the order parameter.

#### Anodization experiments

Recent experiments at Karlsruhe and Argonne<sup>21</sup> indicate that anodization can be an effective way to produce a clean metal-insulator interface between the Nb metal and the Nb<sub>2</sub>O<sub>5</sub> insulator. When Nb is exposed to air a variety of different oxides can form and at least one of these oxides, NbO, is metallic and a superconductor with a transition temperature of about 1.38 K.<sup>20</sup> To produce a surface for which there is a simple boundary condition on the wave function it is important to remove the NbO normal-metal layer and convert it to Nb<sub>2</sub>O<sub>5</sub> insulator. Anodization may provide a way to do this. Nb<sub>2</sub>O<sub>5</sub> has a dielectric constant close to 1 so the Saint James-de Gennes boundary conditions should apply for a Nb-Nb<sub>2</sub>O<sub>5</sub> interface.

To prepare the sample a niobium wire was out-gassed as described earlier and anodized for 20

min at 20 V in a 0.2-N H<sub>2</sub>SO<sub>4</sub> electrolyte. This presumably gives a 400-Å layer of Nb<sub>2</sub>O<sub>5</sub> on the surface of the sample.  $H_{c3}/H_{c2}$  data shown by the solid triangles of Fig. 5 are very close to the un-anodized pure-Nb sample. There is a very slight shift toward the clean limit, so this would seem to indicate that the anodized sample has a cleaner metal-insulator surface than any of the other samples.

#### End effects

A small, but important, experimental detail remains concerning the reproducibility of the susceptibility data from sample to sample. Finnemore *et al.*<sup>12</sup> found that the shape of the  $\mu'$  and  $\mu''$  curves for pure Nb varied a great deal from sample to sample, but this was not the case for samples reported here. In the earlier measurements<sup>12</sup> the samples were about as long as the mutual-inductance coil, whereas in this work the samples were longer than the coils, so there was a good chance that sample-end effects were the cause of the irreproducibility. A series of measurements with the mutual-inductance coils placed at different positions along the sample revealed that a variety of different shaped  $\mu'$  and  $\mu''$  curves similar to those reported earlier could be reproduced by moving the coil near the end of the sample. Hence the lack of reproducibility reported earlier probably arises from end effects.

#### Frequency dependence of $H_{c3}/H_{c2}$

In all the measurements discussed so far, the ac field was set at 31.9 Hz so the measurements might reflect the dynamic response of vortices to time-varying fields. In a way, 31.9 Hz could be considered to be essentially dc because 31.9 Hz is slow compared to the time scale of most superconducting phenomena. Vortices might have important time-delay phenomena, however; so a brief study was made of the frequency dependence of the  $H_{c3}/H_{c2}$  results.

The most prominent effect of frequency changes arises from variations in the normal-state skin depth. For the pure-Nb sample the normal-state skin depth at 31.9 Hz is about 0.9 mm and the radius of the specimen is 0.38 mm, so  $\mu''$  changes radically as the frequency changes from 11 to 11 000 Hz. The change in  $\mu''$  from the superconducting to the normal state was approximately proportional to the square of the frequency, but a detailed study of this effect was not undertaken. The  $\mu'$  curves retain a shape similar to Fig. 2 and these curves were used for the determination of the critical fields.

The most important result of the frequency studies was that  $H_{c1}$  and  $H_{c2}$  are independent of frequency  $f$  as expected, but  $H_{c3}$  increases a small but

measurable amount. The magnitude of the increase is about 5% of  $H_{c2}$  as  $f$  increases from 11 to 11000 Hz and it is essentially independent of temperature. Hence the ratio of  $H_{c3}/H_{c2}$  can be written as the sum of a temperature-dependent term and a frequency-dependent term of the form

$$\frac{H_{c3}}{H_{c2}}(T, f) = \frac{H_{c3}}{H_{c2}}(T, f=1) + 0.015 \log_{10} f.$$

At any given frequency the curves are similar to Fig. 5. The effect of changing the frequency is qualitatively similar to the effect of changing mean free path.

#### SUMMARY

The striking deviations of the ratio of  $H_{c3}/H_{c2}$  from the theory which have been reported earlier have been confirmed for a wide variety of samples, sample surface conditions and normal-state mean

free paths. It is a large effect well outside experimental uncertainty.

A detailed analysis of the temperature dependence of  $H_{c3}/H_{c2}$  near  $T_c$  shows that deviations of the data from the theory diverge as  $(1-t)^{1/2}$ . If the results are fit to a model proposed by Hu, then the data indicate that the effective superconducting interaction constant is depressed by about 1% in a region of about 2 coherence distances at the surface.

#### ACKNOWLEDGMENTS

We would like to thank F. A. Schmidt for preparing the original alloys. John R. Clem made important contributions to this work. One of the authors (J. R. H.) would like to thank the National Aeronautics and Space Administration and National Defense Educational Assistance for financial support during this work.

\*U. S. Atomic Energy Commission Report No. 1S-T-542. This work was performed under Contract No. W-7405-eng-82 with the Atomic Energy Commission.

†Present address: Department of Physics, Oklahoma State University, Stillwater, Okla. 74074.

<sup>1</sup>D. Saint-James and P. G. deGennes, *Phys. Lett.* **7**, 306 (1963).

<sup>2</sup>C. R. Hu and V. Korenman, *Phys. Rev.* **178**, 684 (1969); **185**, 672 (1969).

<sup>3</sup>B. Serin, *Superconductivity*, edited by R. D. Parks (Dekker, New York, 1969), Vol. II, p. 925.

<sup>4</sup>J. E. Ostenson and D. K. Finnemore, *Phys. Rev. Lett.* **22**, 188 (1969).

<sup>5</sup>J. E. Ostenson, J. R. Hopkins, and D. K. Finnemore, *Physica* **55**, 502 (1971).

<sup>6</sup>F. de la Cruz, M. D. Mahoney, and M. Cardona, *Phys. Rev.* **187**, 766 (1969).

<sup>7</sup>R. W. Rollins, R. L. Cappelletti, and J. H. Fearday, *Phys. Rev. B* **2**, 105 (1970).

<sup>8</sup>C. R. Hu, *Phys. Rev.* **187**, 574 (1969).

<sup>9</sup>J. Bardeen, L. N. Cooper, and J. R. Schrieffer, *Phys. Rev.* **108**, 1175 (1957).

<sup>10</sup>W. De Sorbo, *Phys. Rev.* **130**, 2177 (1963); *Phys. Rev.* **132**, 107 (1963); *Phys. Rev.* **134**, A1119 (1964).

<sup>11</sup>E. Fromm and H. Jehn, *Vacuum* **19**, 191 (1969).

<sup>12</sup>D. K. Finnemore, T. F. Stromberg, and C. A. Swenson, *Phys. Rev.* **149**, 231 (1966).

<sup>13</sup>J. R. Hopkins, Ph.D. thesis (Iowa State University, 1972) (unpublished).

<sup>14</sup>R. W. Rollins and J. Silcox, *Phys. Rev.* **155**, 404 (1969).

<sup>15</sup>V. R. Karasik, N. G. Vasil'ev, and V. S. Vrysotskii, *Zh. Eksp. Teor. Fiz.* **62**, 1827 (1973) [*Sov. Phys. JETP* **35**, 945 (1973)].

<sup>16</sup>J. G. Park, *Adv. Phys.* **18**, 103 (1969).

<sup>17</sup>P. G. deGennes, *Superconductivity of Metals and Alloys*, edited by D. Pines (Benjamin, New York, 1966).

<sup>18</sup>J. Auer and H. Ullmaier, *Phys. Rev. B* **7**, 136 (1973).

<sup>19</sup>H. J. Fink and W. C. H. Joiner, *Phys. Rev. Lett.* **23**, 120 (1969).

<sup>20</sup>J. K. Hulm, C. K. Jones, R. A. Hein, and J. W. Gibson, *J. Low Temp. Phys.* **7**, 291 (1972).

<sup>21</sup>K. Gray (private communication).